Polish J. Chem., **76**, 385–394 (2002)

Vibrational Study of the Structural Phase Transitions in a New Ferroelastic $(C_5H_{10}NH_2)SbCl_6$ Crystal by Infrared and Raman Spectroscopies[*]

by B. Bednarska-Bolek[1], R. Jakubas[1], G. Bator[1] and J. Baran[2]**

[1]*Faculty of Chemistry, University of Wrocław, F. Joliot-Curie 14, 50-383 Wrocław, Poland*
[2]*Institute of Low Temperature and Structure Research of the Polish Academy of Science, Okólna 2, 50-950 Wrocław, Poland*

(Received June 28th, 2001; revised manuscript October 19th, 2001)

Infrared spectra of $(C_5H_{10}NH_2)SbCl_6$ in the region of the internal vibrations of the piperidinium cations (3500–400 cm^{-1}) and Raman spectra in the region of internal vibrations of the $SbCl_6^-$ anions (400–100 cm^{-1}), around the phase transitions at $T_{c3} = 294$ K, $T_{c2} = 310$ K and $T_{c1} = 369$ K, are presented and discussed. A detailed analysis has been performed for the bands assigned to the stretching and deformation vibrations of the NH_2^+ and CH_2 groups. It has been shown that the hydrogen bonds play an important role in the mechanism of the phase transitions and influence the dynamics of either cations or anions in different phases of $(C_5H_{10}NH_2)SbCl_6$.

Key words: hexachloroantimonates(V), IR and Raman spectra, phase transition

Molecular-ionic chloroantimonate(V) salts of the formula $RSbCl_6$(V) containing organoammonium cations (R) appear to be an interesting subclass of crystals. They frequently demonstrate ferroelastic phases. Up to now the following ferroic salts belonging to this family have been discovered: $[P(CH_3)_4]SbCl_6$ [1], $[C(NH_2)_3]SbCl_6$ [2], $[(C_2H_5)_3NH]SbCl_6$ [3], $(C_5H_{10}NH_2)SbCl_6{\cdot}(C_5H_{10}NH_2)Cl$ (abbreviation – PCAPC) [4]. The structure of these salts appears to be quite simple. It consists of isolated $SbCl_6^-$ anions and organic cations. The piperidinium analogue (PCAPC) is characterized by slightly more complicated structure, having additionally isolated Cl^- ions.

Very recently we have synthesized simple piperidinium analogue – $(C_5H_{10}NH_2)SbCl_6$ (abbreviated as PCA) [5]. PCA exhibits a rich set of phase transitions:

$$P2_1/m\ (IV) \underset{283\ K}{\overset{294\ K}{\rightleftarrows}} P1\ (III) \underset{310\ K}{\overset{310\ K}{\rightleftarrows}} Cc\ (II) \underset{363\ K}{\overset{369\ K}{\rightleftarrows}} Cmcm\ (I)$$

The ferroelastic domain structure appears below 363 K. The (III→II) phase transition is connected with a change of the conformation of piperidinium cations from chair to twist boat. Furthermore, the contribution of $SbCl_6^-$ groups to the mechanism of the phase transition (III→II) seems to be important. The mechanism of the ferro-paraelastic phase transition (II→I) at 369 K is probably due to the onset of isotropic rotation of the piperidinium cations. The role of both organic cations and

---

[*] Dedicated to the memory of Professor Krzysztof Pigoń

[**] Corresponding author, e-mail: rj@wchuwr.chem.uni.wroc.pl

$SbCl_6^-$ anions in the mechanism of all phase transitions is still unclear. The change in the motional state of these units is expected to influence the internal vibrations of $C_5H_{10}NH_2^+$ cations and $SbCl_6^-$ anions. In order to obtain more information about the molecular mechanism of phase transitions in PCA crystals the vibrational studies (IR and Raman) of the polycrystalline sample in the frequency range 3300–50 cm^{-1} in a wide temperature range have been performed.

EXPERIMENTAL

$(C_5H_{10}NH_2)SbCl_6$ (PCA) has been prepared as described in [5]. Infrared spectra of PCA for the powdered sample in Nujol (NaCl windows) in the temperature range 168–383 K were recorded with a FT-IR spectrometer BRUKER IFS-88 over the frequency range 3300–400 cm^{-1} with resolution 1 cm^{-1}. Specac Variable Temperature Cell P/N 21.500 was used for temperature dependent studies. The temperature of the sample was maintained with an accuracy of ± 0.1 K. IR spectrum of PCA in KBr pellet at room temperature were collected with FT-IR spectrometer BRUKER IFS-113v over the same frequency range with resolution 2 cm^{-1}. It was impossible to perform the temperature dependent IR spectra in KBr pellets, since the replacement of the Cl atoms by the Br ones takes place in the compound studied, especially at high temperatures. Powder FT-Raman spectra were recorded with FRA-106 attachment to the Bruker IFS-88 spectrometer over the frequency range 3300–50 cm^{-1} at room temperature. The temperature studies of Raman spectra of the powdered $(C_5H_{10}NH_2)SbCl_6$ sample were performed using a NICOLET Magna 860 spectrometer with FT Raman Module equipped with an InGaAs detector. The Raman spectra were excited with 1.064 μm radiation from (ND: YVO_4) laser. CaF_2 was used as a beam splitter. The resolution of the Raman spectra was 0.5 cm^{-1} in the region 400–100 cm^{-1}. The home-made sample holder and a UNIPAN 650H temperature controller were used to keep the temperature of the sample with an accuracy of ± 0.5 K.

The program GRAMS/386 Galactic Industries was used for numeral fitting of the experimental data. In order to perform the fitting procedure the absorbance IR spectra were created from the transmission ones. In the case of IR bands only Gaussian function was used for fitting, whereas in the case of Raman spectra the Gaussian·Lorentzian functions product was applied.

RESULTS AND DISCUSSION

The Raman and IR studies of the powdered samples of PCA were performed in the frequency range assigned to the internal vibrations of the piperidinium cation, 3500–400 cm^{-1}, (IR, Raman) and to the internal vibration of the $SbCl_6^-$ anion, 400–100 cm^{-1}, (Raman). The IR spectra were collected in the temperature region between 168 and 383 K. Two IR spectra recorded at extreme temperatures and the Raman spectra at room temperature are shown in Fig. 1. The spectra in the frequency range 3000–2850 cm^{-1}, 1500–1350 cm^{-1} and 740–720 cm^{-1} are not shown (broken line in Fig. 1), because the bands of Nujol appear in these regions. Therefore, the IR spectrum (3300–400 cm^{-1}) in KBr pellets at room temperature was additionally recorded.

The experimental IR and Raman frequencies are collected in Table 1. The tentative assignments of the vibrations are made based on a results reported in: [6,7] – piperidine in aqueous and HCl solutions (in liquid state) and absorbed on silica; [8] – calculated vibrations of piperidine; [9] – piperidine vibrations in solid-state.

Table 1. Wavenumbers (cm^{-1}) and relative intensities of the bands observed in the infrared and Raman spectra of $(C_5H_{10}NH_2)SbCl_6$ (Raman at 295 and 375 K; IR at 168 and 383 K).

IR			Raman	Tentative assignment	IR			Raman		Tentative assignment
168 K (Nujol)	383 K (Nujol)	295 K (KBr)	295 K		168 K (Nujol)	383 K (Nujol)	295 K (KBr)	295 K	375 K	
			3244	ν NH_2^+				1405		δ CH_2
3215 (s,sh)			3227				1387 (m)	1388		
3203 (vs)	3225	3212 (vs)	3209					1376		
3175 (vs)	3195	3187 (vs)	3195				1363 (w)	1362		
			3185							
3154 (s,sh)	3164	3155 (vs,sh)	3168		1347 (w)	1349		1353		ω CH_2
3120 (m,sh)			3148		1331 (w)	1326	1330 (w)	1329		
3109 (s)	3131	3122 (s)						1319		
					1311 (w)	1308	1310 (w)	1309		
		3033 (s)			1300 (m)					
		2998 (s)	2998	ν CH_2	1296 (m)	1293	1296 (w)	1295		
			2983		1283 (vw)		1279 (sh)	1286		
		2967 (s)	2968		1272 (m)	1273	1272 (w)	1276		
		2950 (s)	2952		1269 (sh)			1269		
		2934 (s)	2923					1259		
		2920 (s,sh)								
		2892 (m)	2897		1170 (v)	1169	1171 (vw)	1169		τ CH_2
		2871 (m.)	2876		1157 (m)	1156	1157 (w)	1156		
			2866		1154 (w,sh)	1153				
			2810	combinations and/or overtones transitions	1106 (vw)	1104	1106 (vw)			
			2765							
2737 (sh,w)		2764 (vw)			1075 (m)	1076	1076 (w)	1077		skeletal
2725 (vw)		2724 (vw)	2721		1047 (vw)	1049	1047 (vw)	1046		
2716 (sh)					1033 (w)	1029	1031 (w)			
2700 (vw	2691	2700 (vw)	2695		1026 (m)	1021	1024 (m)	1026		
2672 (vw)					1013 (vs)	1009	1012 (s)	1010		
2659 (vw)			2654							
2629 (vw)					983 (vw)					ρ NH_2^+, CH_2
2616 (vw)					975 (vw)	971				
2594 (vw)	2595	2591 (vw)			962 (vw)					

Table 1 continuation

							946 (sh)			
2564 (vw)		2564 (vw)		combinations and/or overtones transitions	938 (vs)	937	938 (s)			
2549 (vw)					918 (w)	915	915 (vw)			ρ NH_2^+, CH_2
2511 (vw)		2516 (vw)			908 (m)					
2496 (vw)					905 (s)	907	906 (m)			
2477 (vw)	2482	2478 (vw)								
2470 (vw)					889 (w)	892				
2454 (vw)					866 (vw)	865				
2402 (vw)					858 (s)	856	857 (m)	855		
2387 (vw)										
2366 (vw)	2365	2368 (vw)			801 (w)	802	820 (vw)	801		
2360 (vw)					795 (w)	794	798 (w)	792		?
2354 (vw)					770 (vw)	774	773 (vw)			
2343 (vw)							718 (m)			
1815 (vw)							628 (vw)			
1706 (vw)					606 (vw)					
		1646 (vw)			592 (vw)	589				
		1627 (w)			585 (vw)		570 (w)			
		1612 (w)					553 (sh)			
					535 (s)	539	537 (w)			skeletal
1605 (w)		1604 (w)						483		
1601 (w)	1602						453 (vw)	454		
1594 (sh)	1594	1595 (m)					437 (sh)	442		
1574 (sh)				δ NH_2^+				432		
1570 (s)	1577	1574 (s)	1574		427 (s)	426	427 (vw)	424		skeletal
1565 (s)	1564	1565 (sh)								
1548 (vw)	1552							360	348	ν_{as} Sb-Cl
								332	331	ν_s Sb-Cl A_{1g} mode
		1470 (m)	1469					288	286	ν_s Sb-Cl E_g mode
		1458 (sh)						175	173	δ_s Cl-Sb-Cl T_{2g} mode
		1451 (vs)	1453					168		
		1448 (sh)	1441	δ CH_2				117		
		1428 (w)	1431					83		
		1410 (s)	1416							

(vs – very strong, s – strong, m – medium, w – weak, vw – very weak, sh – shoulder, ν - stretching, δ - deformation, ω - wagging, τ - twisting, ρ - rocking)

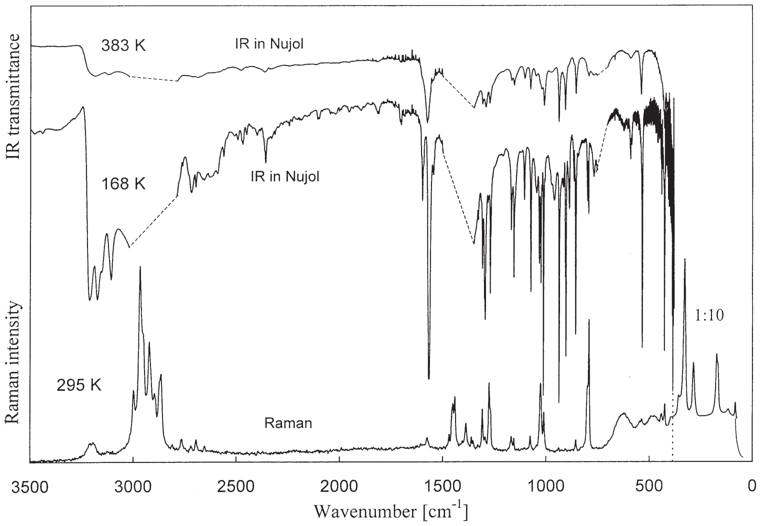

Figure 1. Raman (295 K) and infrared (168 and 374 K) powder spectra of $(C_5H_{10}NH_2)SbCl_6$.

The bands between 3250 and 3100 cm^{-1} are assigned to the stretching vibrations of the NH_2^+ groups, whereas the bands between 3040 and 2860 cm^{-1} are most probably due to the CH_2 stretching modes. The bands observed in the frequency range 1610–1540 cm^{-1} arise from the NH_2^+ deformation modes. The bands between 1470 and 1360 cm^{-1} are assigned to the δ CH_2 scissoring vibrations, whereas the bands between 1350 and 1250 cm^{-1} are assigned to the CH_2 wagging. In the frequency range 1170–1150 cm^{-1} the bands arising from the CH_2 twisting are found. The bands between 1080 and 1010 cm^{-1} and very strong bands at 535 and 427 cm^{-1} are most probably of the skeletal vibration origin. The bands at the frequency range 990–900 cm^{-1} are assigned to the NH_2^+ and CH_2 rocking.

In the Raman spectra the bands between 360 and 70 cm^{-1} are due to the Sb–Cl stretching and the Cl–Sb–Cl deformation modes. Raman temperature studies were performed exclusively in the region 400–100 cm^{-1}.

When the crystal of PCA is heated up from 168 to 383 K, the most spectacular changes in the IR spectra around the phase transition temperatures are found in the NH_2^+ stretching (3300–3050 cm^{-1}) and deformation vibration regions (1620–1540 cm^{-1}). Fig. 2 shows the temperature evolution of the NH_2^+ bands in the IR spectra in above frequency ranges. One can observe that the stretching NH_2^+ band at 3175 cm^{-1} (see Fig. 3a) moves continuously towards higher frequencies with increasing temperature. The shift of this band, by about 20 cm^{-1} in temperature range 168–374 K, is quite large. It was also found that its intensity decreases step-wisely at 294 and 369 K and simultaneously a large broadening of this band is observed (Fig. 3b and c). A shift of the band at 3154 cm^{-1} towards higher frequencies within phase (II) and (I) (Fig. 3a) is accompanied by a small jump of its intensity at the transition temperature, 294 K (Fig. 3b). The remaining bands in this frequency region also move towards higher

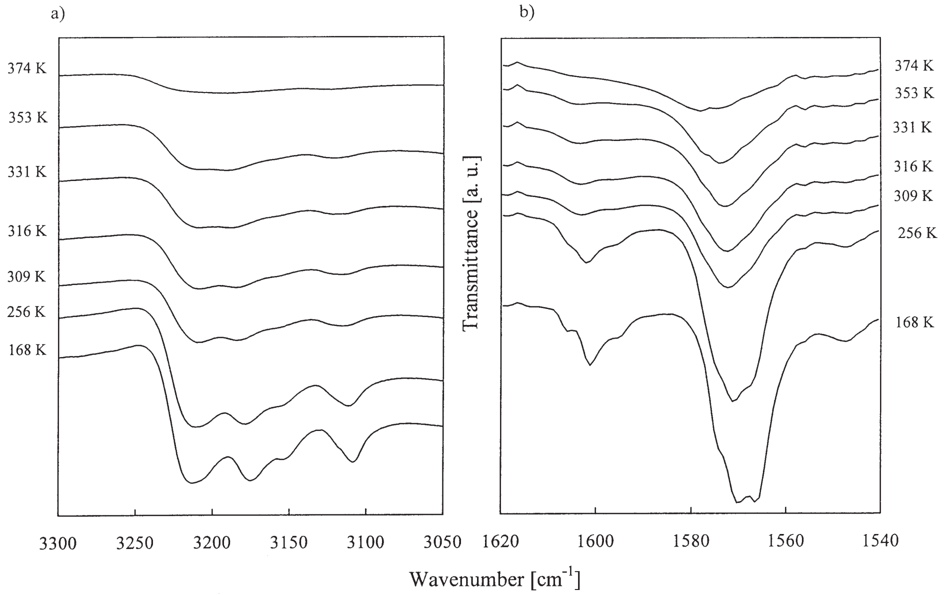

Figure 2. Temperature evolution of the NH_2^+ stretching modes between 3300 and 3050 cm^{-1} (a) and deformation modes between 1620 and 1540 cm^{-1} (b).

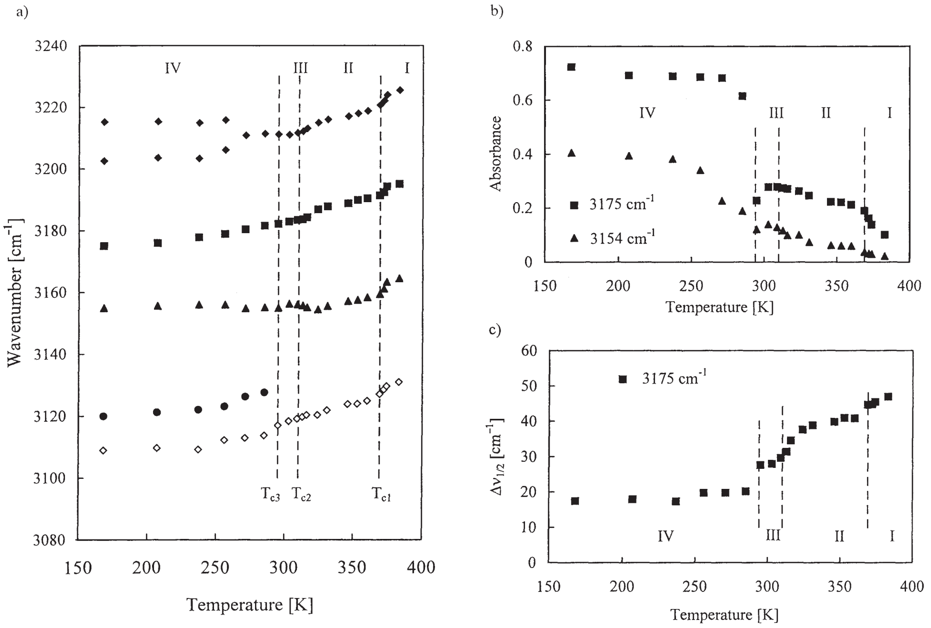

Figure 3. (a) Temperature dependence of the frequencies of the NH_2^+ stretching modes. (b) Temperature dependence of the intensity of the bands at 3154 and 3175 cm^{-1}. (c) Temperature dependence of the bandwidth $\Delta\nu_{1/2}$ of the band at 3175 cm^{-1}.

frequencies and the band at 3120 cm^{-1} disappears at $T_{c3} = 294$ K. Significant changes of the positions of the bands in the deformation NH_2^+ frequency region are observed when the crystal undergoes phase transitions at T_{c3} (Fig. 4). Namely, the bands in the phase (I), at 1577 (383 K) and 1602 cm^{-1} (383 K), split into two components just below the phase transition temperature 294 K (phase IV). The X-ray measurements have revealed that the strength of the hydrogen bonds, N–H....Cl, changes when crystal undergoes the subsequent phase transitions [5]. This situation is clearly reflected in the IR spectra. The bands that arise from the NH_2^+ stretching vibrations move towards higher frequencies, pointing out that the strength of the hydrogen bonds gets weaker at higher temperatures. This effect is usually accompanied by the shift of the bands within NH_2^+ deformation vibrations region towards lower frequencies, which is really seen for the bands at 1565 and 1594 cm^{-1} within phase (II) (see Fig. 4). However, quite opposite effect is seen for the bands at 1548 (168 K) and 1577 cm^{-1} (383 K). It is interesting that when the crystal transforms to the phase (II) the bands mentioned above shift towards higher wavenumbers, which is unexpected effect. Since a

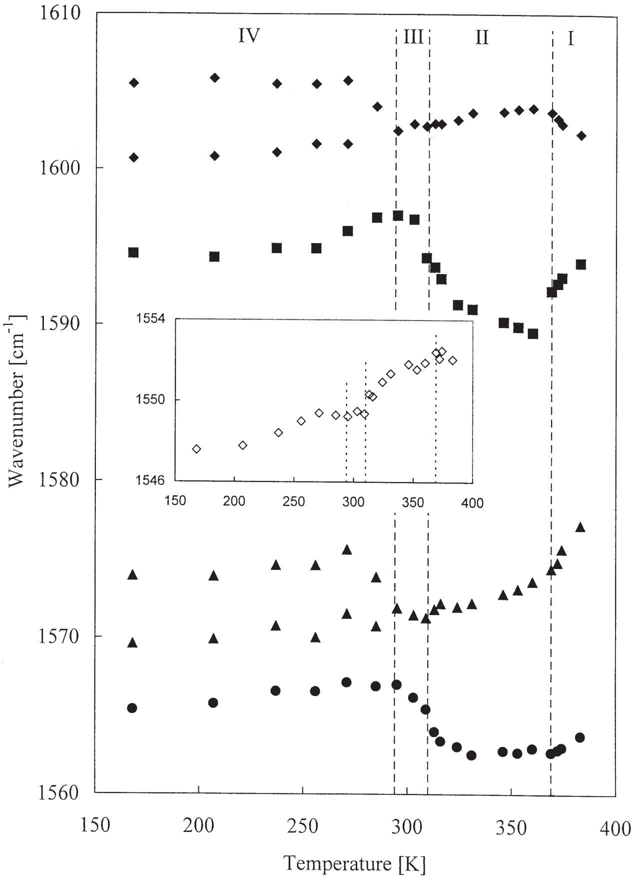

Figure 4. Temperature dependence of the frequencies of the bands in the NH_2^+ deformation region between 1545 and 1610 cm^{-1}.

freedom of reorientation motions of the piperidinium cations and the $SbCl_6^-$ anions are gradually liberated, the bands, which arise from vibrations of the group involved in the hydrogen bonds, get broader and less intensive.

The changes in the dynamics of the piperidinium cations should also influence the changes of the infrared spectra within skeletal vibration region (1075–1010 cm^{-1}). Unexpectedly, these changes are very weak. Nevertheless, in the CH_2 vibration region (1360–1260 cm^{-1}) interesting changes are found, (see Fig. 5a), *i.e.* the bands at 1300 and 1296 cm^{-1} as well as those at 1272 and 1269 cm^{-1} get considerably broader just above T_{c3} = 294 K and form a single band in the phase (III), (see Fig. 5b). The positions of the other bands in this frequency region are almost unchanged with temperature. However, it is clearly seen that their intensities are very sensitive to the changes of the dynamics of cations and significantly decrease above T_{c3} (294 K) and T_{c1} (369 K) (see Fig. 5c) *i.e.* at the first order phase transitions. Additionally, the continuous changes in their absorbance are observed within the phase (II).

Generally, the most spectacular changes in the IR spectra of $(C_5H_{10}NH_2)SbCl_6$ are visible in the vicinity of the phase transition at 294 K as well as over the phase (II) (between 310 and 369 K). Thus, we can conclude that the dynamics of cations and the strength of hydrogen bonds varied mostly when the (IV) → (III) phase transition takes place. It is also clear that the dynamics of piperidinium cations changes significantly over the phase (II) in a continuous way.

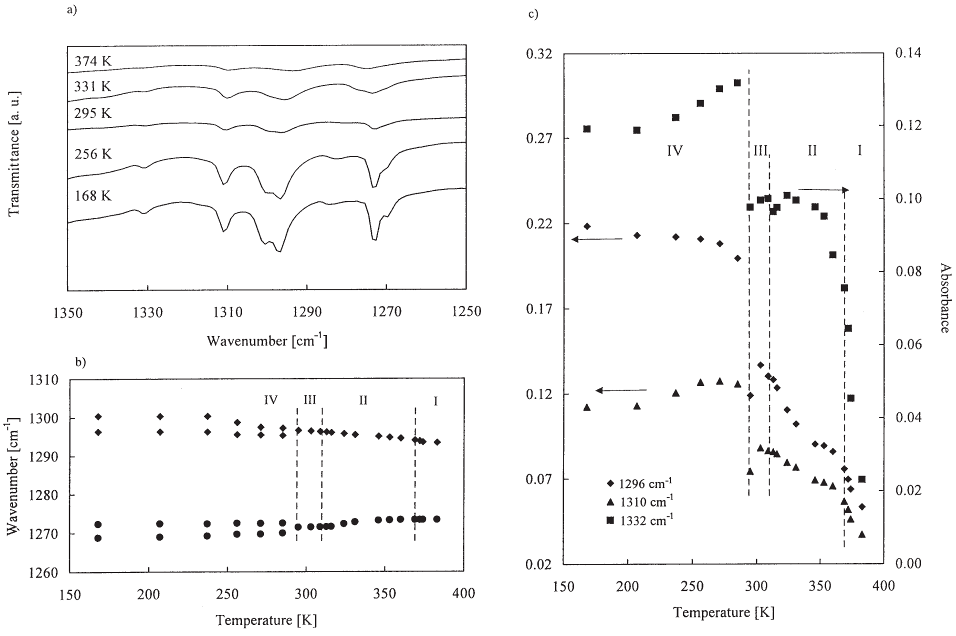

Figure 5. (a) Temperature evolution of the CH_2 deformation modes between 1350 and 1250 cm^{-1}. (b) Temperature dependence of the frequencies of these modes. (c) Temperature dependence of the intensity of the bands at 1296, 1310 and 1332 cm^{-1}.

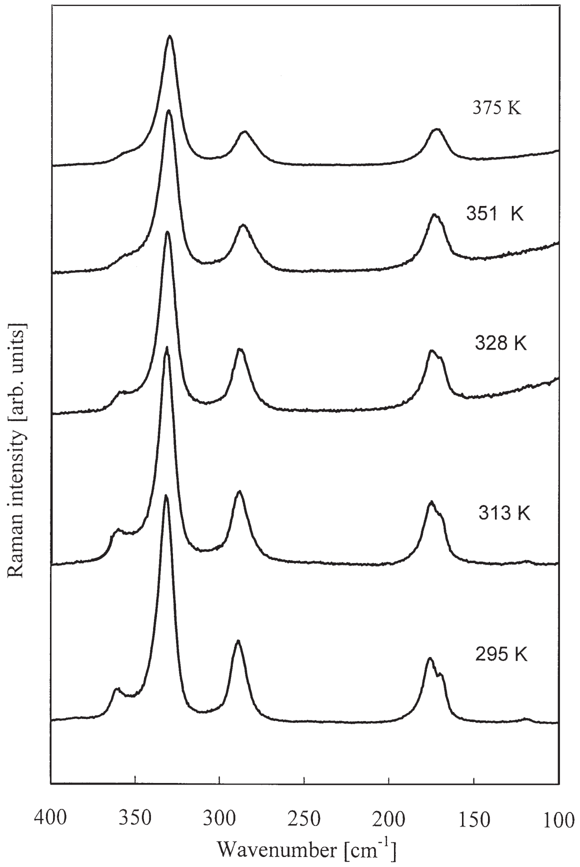

Figure 6. Temperature evolution of the Raman spectra in the internal vibration region of $SbCl_6^-$ anions.

The temperature X-ray experiment indicated a considerable role of the anionic sublattice in the mechanism of the phase transitions encountered in PCA [5]. Therefore, the Raman spectra, in the frequency range 400–100 cm^{-1}, assigned to the internal vibrations of $SbCl_6^-$ anions, between 295 and 375 K were collected. For the sake of experimental conditions the Raman spectra were not investigated below the (IV→III) phase transition at 294 K. Fig. 6 displays the temperature evolution of Raman spectra in that frequency region. The bands assigned to the Sb–Cl stretching and Cl–Sb–Cl deformation vibrations generally do not change their positions, but their strong broadening at T_{c2} is distinctly observed over the phase (II), especially for the bands at 360 and 288 cm^{-1} (Fig. 7a and b). This situation in the Raman spectra probably reflects the liberation of reorientational motions of the $SbCl_6$ octahedra in this phase. In the highest temperature phase (I), the further broadening of these bands may be explained in terms of the isotropic rotational motion of the $SbCl_6^-$ anions.

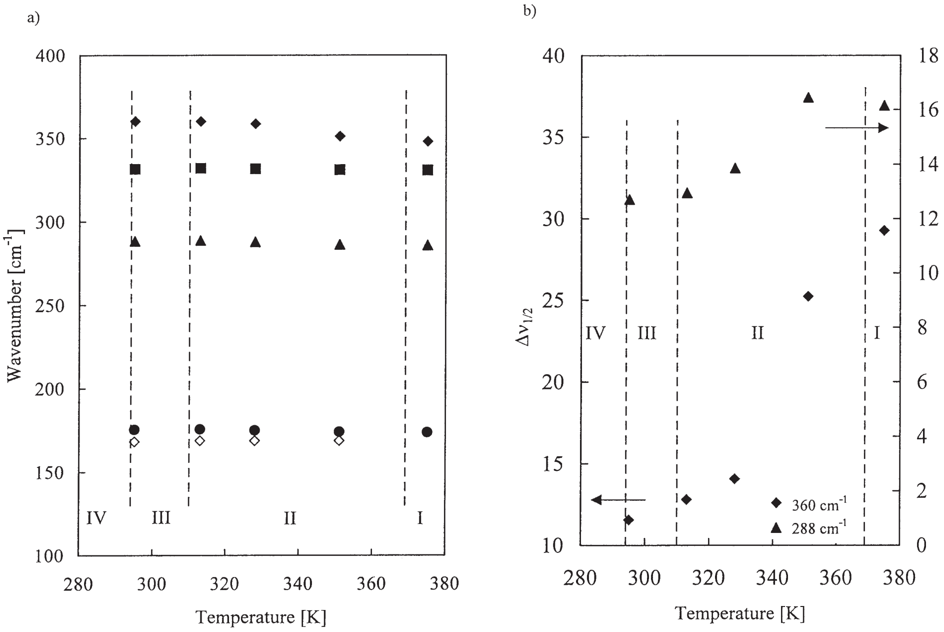

Figure 7. (a) Temperature dependence of the frequencies of the Sb–Cl stretching and Cl–Sb–Cl deformation modes between 100–400 cm^{-1}. (b) Temperature dependence of the bandwidths $\Delta\nu_{1/2}$ of the bands in this region.

Acknowledgment

This work was supported by the Polish State Committee for Scientific Research (project register 3 T09A 058 17).

REFERENCES

1. Ciąpała P., Jakubas R., Bator G., Pietraszko A. and Kosturek B., *J. Phys.: Condens. Matter*, **10**, 5439 (1998).
2. Jakubas R., Ciąpała P., Pietraszko A., Zaleski J. and Kusz J., *J. Phys. Chem. Sol.*, **59**, 1309 (1998).
3. Bednarska-Bolek B., Pietraszko A., Jakubas R., Bator G. and Ciąpała P., *J. Phys. Chem. Sol.*, (2001) in press.
4. Bednarska-Bolek B., Pietraszko A., Jakubas R., Bator G. and Kosturek B., *J. Phys.: Condens. Matter*, **12**, 1143 (2000).
5. Pietraszko A., Bednarska-Bolek B., Jakubas R. and Zieliński P., *J. Phys.: Condens. Matter*, **13**, 6471 (2001).
6. Hirokawa T., Kimura T, Murata H. and Ohno K., *Spectrochim. Acta,* **36A**, 329 (1980).
7. Nguyen T.T., Curthoys G.C. and Cooney R.P., *Appl. Spectrosc.*, **27**, 484 (1973).
8. Vlasowa T.F. and Sheinker Yu.N., *Zh. Prikl. Spektrosk.*, **14**, 657 (1971).
9. Cariati F., Marcotrigiano G., Menabue L., Morazzoni F., Pellacani G.C. and Zanderighi G.M., *Spectrochim. Acta*, **34A**, 801 (1978).